Optics Communications 281 (2008) 5083–5091

Contents lists available at ScienceDirect

Optics Communications

journal homepage: www.elsevier.com/locate/optcom

Effects of coherence and polarization changes on the heterodyne detection of stochastic beams propagating in free space

Mohamed Salem *, Jannick P. Rolland

CREOL, The College of Optics and Photonics, University of Central Florida, 4000 Central Florida Blvd., Orlando, Fl 32816, United States

ARTICLE INFO

Article history:
Received 11 October 2007
Received in revised form 5 June 2008
Accepted 1 July 2008

Keywords:
Heterodyne detection
Random electromagnetic beams
Signal-to-noise ratio

ABSTRACT

We evaluate the heterodyne efficiency of a heterodyne (coherent) detection system for partially polarized, partially coherent, quasi-monochromatic beams. The beam-coherence-polarization (BCP) matrix is used for the description of the statistical ensemble of this class of stochastic beams. We investigate the dependence of the efficiency of the detection process on the beams parameters as the beams propagate in free space. We discuss how the optimization of the detection system can be performed for received beams with different coherence and polarization properties by adjusting the corresponding properties of the local oscillator beam. The dependence of the mixing efficiency on the size of the receiving aperture is emphasized. We derive an analytical expression for the heterodyne efficiency in the case when both the received beam and the local oscillator beam belong to a broad class of so-called electromagnetic Gaussian Schell-model beams. Our analysis is illustrated by numerical examples.

1. Introduction

Optical heterodyne (coherent) detection is a powerful technique for the detection of weak signals or signals which are embedded into strong incoherent backgrounds [1,2], because in such situations it can perform much better compared with a direct (incoherent) detection [3]. The heterodyne detection system is characterized by its capability of noise reduction and by its high spectral resolution [4,5]. Because of these advantages it has been extensively studied from different perspectives (see, for example, [6,7]).

In order to estimate the performance of a heterodyne detection system one conventionally uses the signal-to-noise ratio (SNR) as a measure for the capability of the system to reject the noise inherent in it or the heterodyne efficiency as a metric to measure the mixing efficiency of the two overlapped beams on the detector surface. Fink [8] derived a general expression for the SNR and heterodyne efficiency of heterodyne detection of *coherent beams*, in terms of the intensity distributions of the mixed beams across the detector surface, taking into account the size and the shape of the detector as well. Lathi [9] derived an expression for the SNR for two linearly polarized, partially coherent beams, which are mixed on a detector surface; later Lathi and Nagel [10] also gave optimization criteria for the choice of the parameters of the local oscillator beam, which maximizes the SNR when detecting such a beam. Recently, Salem and Dogariu [11] obtained an expression for the SNR when partially polarized, partially coherent beams are detected coherently. In [11], however, only a special case was treated in details, namely, when the mixed beams have uniform polarization across the detector surface. The heterodyne efficiency has been considered as a measure of quality of a heterodyne detection system to evaluate the performance of the coherent detection technique compared with the incoherent scheme [12]. It has been considered also to be a measure of the misalignment between the received beam and the locally generated one in coherent detection systems [13]. The heterodyne efficiency of a coherent detection system has been discussed in many publications in connection with the evaluation of the performance of coherent detection systems. For example Cohen [14] examined the effects of the phase-front misalignment between detected overlapped beams on the mixing efficiency. He studied the case of mixing fully coherent beams for different distributions of the beams intensity. Tanaka and Ohta [15] have studied the effect of the tilt and the offset of the received signal on the heterodyne efficiency of Gaussian beams and Tanaka and Saga obtained optimal conditions for the maximum heterodyne efficiency in coherent detection systems in the presence of background radiation [16]. Recently Salem studied the problem of coherently mixing two partially coherent beams with a small phase shift between their wave vectors, which reflect on the misalignment of the two beams [17]. The author emphasized the effect of this slight phase difference on the heterodyne detection of beams of any state of coherence.

It has been shown relatively recently that the coherence and the polarization properties of, quasi-monochromatic stochastic electromagnetic beams can appreciably change as the beam

* Corresponding author. Tel.: +1 4076902520.
E-mail address: msalem@creol.ucf.edu (M. Salem).

0030-4018/$ - see front matter © 2008 Elsevier B.V. All rights reserved.
doi:10.1016/j.optcom.2008.07.015

propagates, even in free space (cf. [18]). Moreover, the polarization of the beam can vary not only along the propagation distance but also in a direction perpendicular to it. Hence, even if the beam is generated with certain polarization properties, (usually being uniform across the transverse plane), after propagation, it will generally have somewhat different (and, moreover, usually not uniform) polarization properties across the surface of the detector.

In this paper we generalize the definition of the heterodyne efficiency, given in Ref. [17] for scalar beams, to stochastic electromagnetic beams based upon the definition for the detected power of a heterodyne system of stochastic electromagnetic beams provided in [11]. We study the detection of beams propagating in free space from a remote source to a detector surface. Moreover, in order to carry out the most complete optimization of the detection system we will consider that the locally generated beam, akin the received beam, might also propagate a certain distance to the detector surface. The aim of this paper is to examine how the heterodyne efficiency of the system varies, not only with the size of the detector and the polarization properties of the mixed beams, but also with the propagation distances. Whilst the parameters of the received beam are not known, those of the local oscillator beam are fully controllable. We will show that the parameters of the local oscillator and the detector size can be chosen to maximize the mixing efficiency of the detection system.

The paper is organized as follows: in Section 2 we review free-space propagation of quasi-monochromatic, partially polarized beams of any state of coherence emphasizing the evolution of the polarization properties of the beam across its cross-section when the propagation distance increases. We will consider the propagation of a particular class of beams, the so-called electromagnetic Gaussian Schell-model (GSM) beams. In Section 3 we introduce the heterodyne detection system in which both the received beam and the local oscillator beam are partially polarized, partially coherent, quasi-monochromatic beams, which reach the detector surface after free-space propagation from their generating sources. In Section 4 we apply the definition of the heterodyne efficiency of a coherent system when the mixed beams are electromagnetic Gaussian Schell-model beams. We derive an analytical expression for the heterodyne efficiency when two electromagnetic GSM are combined coherently. Finally, in Section 5 we show by some numerical examples how different parameters of the beams affect the mixing efficiency in a coherent detection system. The optimization of the detection can be made by adjusting the size of the detector aperture and the properties of the local oscillator beam.

2. Free-space propagation of a stochastic electromagnetic beam

We begin by giving a brief review for the free-space propagation of quasi-monochromatic partially polarized, partially coherent beams and we examine how the intensity and the polarization through the cross-section of the beam in the transverse direction, change with increasing propagation distance. As we will see in Section 5, such changes have important implications on the detection system.

Suppose that the source is located in the plane $z = 0$ and generates a quasi-monochromatic, partially polarized, partially coherent beam propagating close to the positive z direction (see Fig. 1). The statistical ensemble of such a stochastic beam can be defined in terms of second-order correlation properties of the beam in the source plane using the so-called beam-coherence-polarization (BCP) matrix [19]

$$\mathbf{J}(\boldsymbol{\rho}_1', \boldsymbol{\rho}_2', 0) = \begin{pmatrix} J_{xx}(\boldsymbol{\rho}_1', \boldsymbol{\rho}_2', 0) & J_{xy}(\boldsymbol{\rho}_1', \boldsymbol{\rho}_2', 0) \\ J_{yx}(\boldsymbol{\rho}_1', \boldsymbol{\rho}_2', 0) & J_{yy}(\boldsymbol{\rho}_1', \boldsymbol{\rho}_2', 0) \end{pmatrix}. \tag{2-1}$$

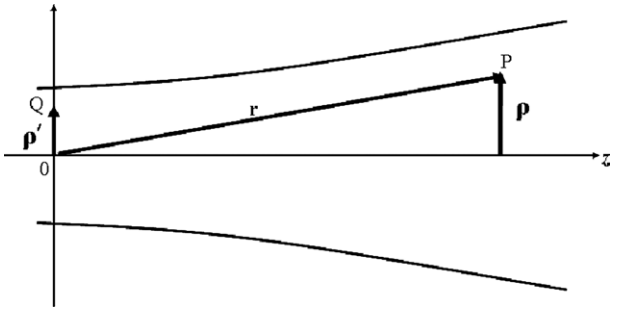

Fig. 1. Illustrating notation relating to the propagation of a beam in free space.

The elements of this matrix are the correlation functions between the mutually orthogonal components of the electric field, $E_x(\boldsymbol{\rho}', 0)$ and $E_y(\boldsymbol{\rho}', 0)$, at points with transverse position vectors $\boldsymbol{\rho}_1'$ and $\boldsymbol{\rho}_2'$ in the source plane at the same instant of time, i.e.,

$$J_{ij}(\boldsymbol{\rho}_1', \boldsymbol{\rho}_2', 0) = \langle E_i^*(\boldsymbol{\rho}_1', 0) E_j(\boldsymbol{\rho}_2', 0) \rangle, \quad (i,j = x,y), \tag{2-2}$$

where the asterisk denotes the complex conjugate and the angular brackets denote the ensemble average. The elements of the BCP matrix of the beam $[J_{ij}(\boldsymbol{\rho}_1, \boldsymbol{\rho}_2, z)]$, at distance z from the source plane, can be calculated from the corresponding elements of the BCP matrix defined by Eqs. (2-1) and (2-2), i.e., $J_{ij}(\boldsymbol{\rho}_1', \boldsymbol{\rho}_2', 0)$, using the propagation laws (cf. Ref. [20]) within the assumption of the paraxial approximation

$$\begin{aligned} J_{ij}(\boldsymbol{\rho}_1, \boldsymbol{\rho}_2, z) = \frac{1}{\lambda^2 z^2} \int\int & J_{ij}(\boldsymbol{\rho}_1', \boldsymbol{\rho}_2', 0) \\ & \times \exp\left\{ -\frac{ik}{2z} [(\boldsymbol{\rho}_1 - \boldsymbol{\rho}_1')^2 - (\boldsymbol{\rho}_2 - \boldsymbol{\rho}_2')^2] \right\} \mathrm{d}^2\rho_1' \, \mathrm{d}^2\rho_2', \\ & (i,j) = (x,y), \end{aligned} \tag{2-3}$$

where $k = 2\pi/\lambda$ is the wave number of the beam, λ is the central wavelength of the quasi-monochromatic wave and the integration extends over the source domain.

We will now assume that the source generates the so-called electromagnetic Gaussian Schell-model (GSM) beam. Following Ref. [20], the components of the BCP matrix characterizing such a beam in the plane of the source are given by the expressions

$$J_{ij}(\boldsymbol{\rho}_1', \boldsymbol{\rho}_2', 0) = I_{ij} \exp\left[-\frac{(\boldsymbol{\rho}_1'^2 + \boldsymbol{\rho}_2'^2)}{4\sigma^2} \right] \exp\left[-\frac{(\boldsymbol{\rho}_2' - \boldsymbol{\rho}_1')^2}{2\delta_{ij}^2} \right], \quad (i,j = x,y), \tag{2-4}$$

where I_{ij} are the on-axis intensities, σ is the r.m.s. width of the beam, δ_{ij} are the r.m.s. widths of the correlations. On substituting from Eq. (2-4) into Eq. (2-3) and performing the integration one obtains for the elements of the BCP matrix of the beam in the detector plane the expressions [19]

$$\begin{aligned} J_{ij}(\boldsymbol{\rho}_1, \boldsymbol{\rho}_2, z) = \frac{I_{ij}}{A_{ij}^2(z)} & \exp\left(-\frac{\boldsymbol{\rho}_1^2 + \boldsymbol{\rho}_2^2}{4\sigma^2 A_{ij}^2(z)} \right) \exp\left(-\frac{(\boldsymbol{\rho}_1 - \boldsymbol{\rho}_2)^2}{2\delta_{ij}^2 A_{ij}^2(z)} \right) \\ & \times \exp\left(-\frac{ik(\boldsymbol{\rho}_1^2 - \boldsymbol{\rho}_2^2)}{2R_{ij}(z)} \right). \end{aligned} \tag{2-5}$$

Here the beam expansion coefficients $A_{ij}^2(z)$ and the curvature coefficients $R_{ij}(z)$ are given by the formulas

$$A_{ij}^2(z) = 1 + \left(\frac{z}{k\sigma} \right)^2 \left(\frac{1}{4\sigma^2} + \frac{1}{\delta_{ij}^2} \right), \tag{2-6}$$

$$R_{ij}(z) = z\left(1 + \frac{1}{A_{ij}^2(z)} \right). \tag{2-7}$$

Now, we will examine the variation of the intensity and of the polarization properties of the beam with distancezof propagation. The intensity of the beam at a point P, which is defined by the vector, $\mathbf{r} = (\boldsymbol{\rho}, z)$ is given by the expression

$$I(\boldsymbol{\rho}, z) = \mathrm{Tr}\mathbf{J}(\boldsymbol{\rho}, z), \tag{2-8}$$

where Tr denotes the trace. The polarization properties of the beam consist of the degree of polarization and the state of polarization of the beam. The degree of polarization of the beam is defined by the formula [20]

$$P(\boldsymbol{\rho}, z) = \sqrt{1 - \frac{4\mathrm{Det}\mathbf{J}(\boldsymbol{\rho}, z)}{[\mathrm{Tr}\mathbf{J}(\boldsymbol{\rho}, z)]^2}}, \quad 0 \leqslant P \leqslant 1, \tag{2-9}$$

where Det denotes the determinant. The state of polarization at any point within the beam cross-section is characterized by the parameters specifying the polarization ellipse (cf. [21]) which can be determined from the BCP matrix. The orientation angle θ of the polarization ellipse, i.e., the angle which the major axis of the polarization ellipse makes with the x-direction, is given by the formula (cf. [22])

$$\theta(\boldsymbol{\rho}, z) = \frac{1}{2}\arctan\left(\frac{2\mathrm{Re}[J_{xy}(\boldsymbol{\rho}, z)]}{J_{xx}(\boldsymbol{\rho}, z) - J_{yy}(\boldsymbol{\rho}, z)}\right), \quad -\pi/2 \leqslant \theta \leqslant \pi/2. \tag{2-10}$$

The degree of ellipticity of the polarization ellipse can be defined by the formula [22]

$$\varepsilon(\boldsymbol{\rho}, z) = A_2(\boldsymbol{\rho}, z)/A_1(\boldsymbol{\rho}, z), \quad 0 \leqslant \varepsilon \leqslant 1, \tag{2-11}$$

where $A_1(\boldsymbol{\rho}, z)$ and $A_2(\boldsymbol{\rho}, z)$ are the magnitudes of the major and of the minor semi-axes of the polarization ellipse respectively, given by the expressions

$$A_1(\boldsymbol{\rho}, z) = \left(\sqrt{(J_{xx} - J_{yy})^2 + 4|J_{xy}|^2} + \sqrt{(J_{xx} - J_{yy})^2 + 4[\mathrm{Re}J_{xy}]^2}\right)^{1/2} \Big/ \sqrt{2}, \tag{2-12a}$$

$$A_2(\boldsymbol{\rho}, z) = \left(\sqrt{(J_{xx} - J_{yy})^2 + 4|J_{xy}|^2} - \sqrt{(J_{xx} - J_{yy})^2 + 4[\mathrm{Re}J_{xy}]^2}\right)^{1/2} \Big/ \sqrt{2}. \tag{2-12b}$$

In Eqs. (12) the arguments of the BCP matrix elements have been omitted for simplicity. The degree of ellipticity $\varepsilon(\boldsymbol{\rho}, z)$ characterizes the shape of polarization ellipse; it is unity for circular polarization and zero for linear polarization.

In Fig. 2 we give an example for the variation of the intensity, the degree of polarization and the orientation angle of a stochastic electromagnetic beam versus the propagation distance z from the plane of the source and also the transverse distance $\boldsymbol{\rho}$ from the axial point of the beam as given by Eqs. (2-8)–(2-10). It was assumed that the propagating stochastic beam was generated by a linearly polarized Gaussian Schell-model source that has the parameters $I_{xx} = 2.25$, $I_{yy} = 1$, $\sigma = 1$ cm, $\delta_{xx} = 0.15$ mm, $\delta_{yy} = 0.225$ mm, $\delta_{xy} = 0.25$ mm and $I_{xy} = 0.45$. From the contour plots one can readily see that, as the beam propagates sufficiently far from the source plane, its intensity distribution and also the distributions of its polarization properties change, and they are becoming non-uniform across the beam cross-section. This non-uniformity will impact the required properties of the local oscillator beam and the detector size. Also, since in a typical detection system the distance that the detected beam propagates from its source, say z_S, is sufficiently large, i.e., $z_S/\lambda \gg 1$ (the detected beam is in its far zone), both its intensity and the polarization properties of the beam are affected by propagation (they are redistributed across the detector surface). Therefore, in general, the local oscillator beam at the detector surface should also exhibit far-zone characteristics, i.e., the distance between its source and the detector;

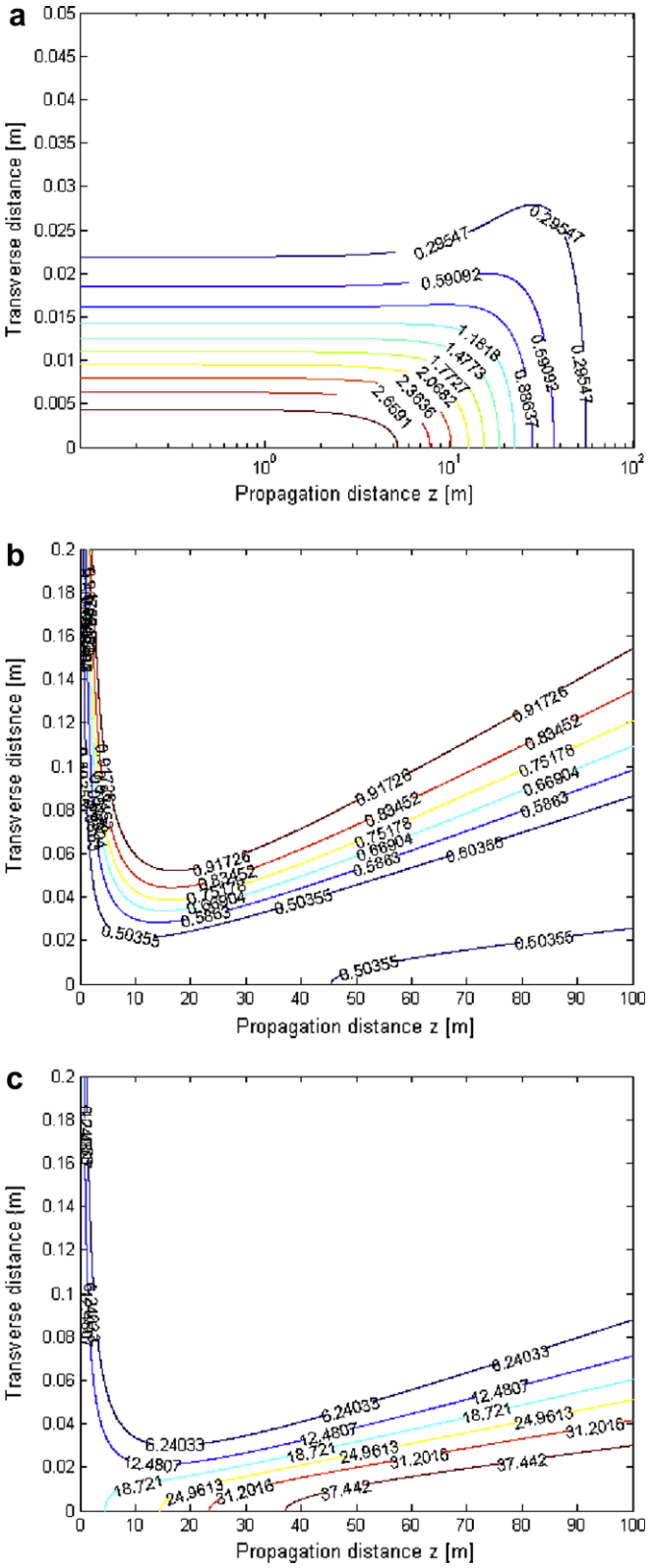

Fig. 2. Contour plots for the variation of (a) the intensity of the beam (b) the degree of polarization of the beam (c) the changes in the orientation angle, of a linearly polarized beam versus the propagation and the transverse distances of a beam propagating in free space. The parameters of the beam were taken as $\lambda = 0.6328$ μm, $I_{xx} = 2.25$, $I_{yy} = 1$, $\sigma = 1$ cm, $\delta_{xx} = 0.15$ mm, $\delta_{yy} = 0.225$ mm, $\delta_{xy} = 0.25$ mm and $I_{xy} = 0.45$.

say z_L should be sufficiently large, viz. $z_L/\lambda \gg 1$ in such a way that the parameters of the local oscillator beam should match the corresponding parameters of the received beam after propagating a distance z_S from the source plane. In other words, the detection system might be considered as having allowed (controllable) propagation path between the local oscillator and the detector plane. Such a system will now be introduced and analyzed.

3. Heterodyne detection of stochastic electromagnetic beams

A schematic diagram for the analyzed detection system is shown in Fig. 3. Two acousto-optics modulators AOM1 and AOM2 can be used to modulate the optical beams with angular frequencies ω_S and ω_L in the radio frequency (RF) range. C1 and C2 denote the generators of the random beams, which can be realized according to the methods proposed by Piquero et al. [23] or Shirai et al. [24]. Hence, the output of the generators C1 and C2 can be characterized by the BCP matrices of the correlation pairs with frequencies $\omega + \omega_S$ and $\omega + \omega_L$, where ω denotes the optical angular frequency. Suppose that the distances, which the two beams, the received and the local oscillator beams, travel to the detector from generators C1 and C2 are z_S and z_L, respectively. The expression for the signal-to-noise ratio (SNR) of the coherent mixing of stochastic electromagnetic beams, is given in [11] as

$$\mathrm{SNR} = \frac{2\mathrm{Re}\int_D \Re(\boldsymbol{\rho_1})\Re(\boldsymbol{\rho_2})\mathrm{Tr}[\mathbf{J}^{(S)\dagger}(\boldsymbol{\rho_1},\boldsymbol{\rho_2},z_S)\mathbf{J}^{(L)}(\boldsymbol{\rho_1},\boldsymbol{\rho_2},z_L)]\,\mathrm{d}^2\rho_1\,\mathrm{d}^2\rho_2}{2eB\int_D \Re(\boldsymbol{\rho})\mathrm{Tr}[\mathbf{J}^{(L)}(\boldsymbol{\rho},\boldsymbol{\rho},z_L)]\,\mathrm{d}^2\rho}. \tag{3-1}$$

where $\mathbf{J}^{(S)}(\boldsymbol{\rho_1},\boldsymbol{\rho_2},z_S)$ and $\mathbf{J}^{(L)}(\boldsymbol{\rho_1},\boldsymbol{\rho_2},z_L)$ are the BCP matrices of the detected beam and the local oscillator beam at the surface of the detector, Re denotes the real part and dagger denotes the Hermitian adjoint. In Eq. (3-1), e is the electron charge, B is the bandwidth of the intermediate frequency (IF) filter and $\Re(\boldsymbol{\rho})$ is the responsivity of the detector at the position $\boldsymbol{\rho}$ on the detector surface. Eq. (3-1) can be modified to take into account any misalignment between the wave-fronts of the two overlapped beams on the detector as given in [17] hence it can be expressed as

$$\mathrm{SNR} = \frac{\int_D 2\mathrm{Re}\Re(\boldsymbol{\rho_1})\Re(\boldsymbol{\rho_2})\mathrm{Tr}[\mathbf{J}^{(S)\dagger}(\boldsymbol{\rho_1},\boldsymbol{\rho_2},z_S)\mathbf{J}^{(L)}(\boldsymbol{\rho_1},\boldsymbol{\rho_2},z_L)]\exp(j\mathbf{K}\cdot\boldsymbol{\rho_1}-j\mathbf{K}\cdot\boldsymbol{\rho_2})\,\mathrm{d}^2\rho_1\,\mathrm{d}^2\rho_2}{2eB\int_D \Re(\boldsymbol{\rho})\mathrm{Tr}[\mathbf{J}^{(L)}(\boldsymbol{\rho},\boldsymbol{\rho},z_L)]\,\mathrm{d}^2\rho}, \tag{3-2}$$

where $\mathbf{K}$ is the wave vector of the received signal, assuming that the local oscillator is propagating in a direction normal to the detector as shown in Fig. 4. Sometimes it is more appropriate to define a normalized SNR, a quantity that does not depend on the detector parameters in general but depends on the parameters of the overlapped beams only. For stochastic electromagnetic beams mixing one can define the normalized SNR by the formula

$$\mathrm{SNR}^* = \frac{\int_D \mathrm{ReTr}[\mathbf{J}^{(S)\dagger}(\boldsymbol{\rho_1},\boldsymbol{\rho_2},z_S)\mathbf{J}^{(L)}(\boldsymbol{\rho_1},\boldsymbol{\rho_2},z_L)]\exp(j\mathbf{K}\cdot\boldsymbol{\rho_1}-j\mathbf{K}\cdot\boldsymbol{\rho_2})\,\mathrm{d}^2\rho_1\,\mathrm{d}^2\rho_2}{\int_D \mathrm{Tr}[\mathbf{J}^{(L)}(\boldsymbol{\rho},\boldsymbol{\rho},z_L)]\,\mathrm{d}^2\rho}, \tag{3-3}$$

where we assumed that the responsivity does not vary with the position on the detector. Then $\Re(\boldsymbol{\rho}) = \Re = \frac{e\eta_q}{h\upsilon}$ at different positions, where η_q is the quantum efficiency of the photo-surface, h is the Planck's constant, and υ is the optical frequency [1]. We note that the normalized SNR has the units (J Hz) and does not depend on some of the detector parameters.

To evaluate the performance of the coherent detection system in this case and to show the effect of the variation of different parameters on the detection process, it is convenient to use the heterodyne efficiency as a metric for the quality of the system. Following the same procedure as in [17] one could extend the definition of the heterodyne efficiency to the case of stochastic electromagnetic beams to be written in the form

$$\eta_h = \frac{\int_D \int_D \mathrm{Re}\Re(\boldsymbol{\rho_1})\Re(\boldsymbol{\rho_2})\mathrm{Tr}[\mathbf{J}^{(S)\dagger}(\boldsymbol{\rho_1},\boldsymbol{\rho_2},z_S)\mathbf{J}^{(L)}(\boldsymbol{\rho_1},\boldsymbol{\rho_2},z_L)]\exp(j\mathbf{K}\cdot\boldsymbol{\rho_1}-j\mathbf{K}\cdot\boldsymbol{\rho_2})\,\mathrm{d}^2\rho_1\,\mathrm{d}^2\rho_2}{\int_D \Re(\boldsymbol{\rho})\mathrm{Tr}[\mathbf{J}^{(L)}(\boldsymbol{\rho},\boldsymbol{\rho},z_L)]\,\mathrm{d}^2\rho \cdot \int_D \Re(\boldsymbol{\rho})\mathrm{Tr}[\mathbf{J}^{(S)}(\boldsymbol{\rho},\boldsymbol{\rho},z_S)]\,\mathrm{d}^2\rho}. \tag{3-4}$$

This equation reduces to the corresponding equation of the scalar beams mixing demonstrated in [17] when it has been applied to the scalar beams mixing. Eq. (3-4) has maximum value when two co-aligned fully polarized electromagnetic beams are mixed together. Assuming that the responsivity is constant across the detector, the corresponding expression for the heterodyne efficiency of the electromagnetic beams can be defined by the formula

$$\eta_h = \frac{\int_D \int_D \mathrm{ReTr}[\mathbf{J}^{(S)\dagger}(\boldsymbol{\rho_1},\boldsymbol{\rho_2},z_S)\mathbf{J}^{(L)}(\boldsymbol{\rho_1},\boldsymbol{\rho_2},z_L)]\exp(j\mathbf{K}\cdot\boldsymbol{\rho_1}-j\mathbf{K}\cdot\boldsymbol{\rho_2})\,\mathrm{d}^2\rho_1\,\mathrm{d}^2\rho_2}{\int_D \mathrm{Tr}[\mathbf{J}^{(L)}(\boldsymbol{\rho},\boldsymbol{\rho},z_L)]\,\mathrm{d}^2\rho \cdot \int_D \mathrm{Tr}[\mathbf{J}^{(S)}(\boldsymbol{\rho},\boldsymbol{\rho},z_S)]\,\mathrm{d}^2\rho}. \tag{3-5}$$

From Eqs. (3-3) and (3-5) one can relate the heterodyne efficiency to the normalized SNR, when the responsivity of the detector does not depend on the position, by the formula

$$\eta_h = \frac{\mathrm{SNR}^*}{\int_D \mathrm{Tr}[\mathbf{J}^{(S)}(\boldsymbol{\rho},\boldsymbol{\rho},z_s)]\,\mathrm{d}^2\rho}. \tag{3-6}$$

As is evident from Eq. (3-5) the heterodyne efficiency can also be regarded as representing reduction of the optimum incoherent power upon mixing two beams coherently on a detector surface [25]. In the next section we give an analytical solution for this equation when the two overlapping beams belong to the broad class of Gaussian Schell-model (GSM).

4. Heterodyne detection of partially polarized Gaussian Schell-model beams

When both the received beam and the local oscillator beam belong to a class of partially polarized, Gaussian Schell-model beams [20], an expression for the heterodyne efficiency can readily be derived. Suppose that the BCP matrices of the detected beam and the local oscillator beam at the detector surface have the elements (see Eqs. (2-5)–(2-7))

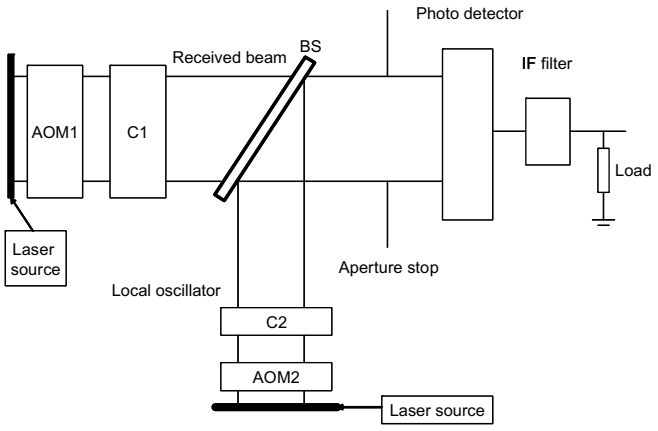

Fig. 3. Schematic diagram for the heterodyne detection system. Different symbols are explained in the text.

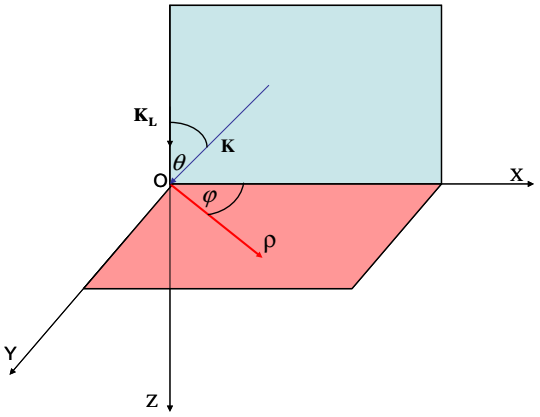

Fig. 4. Illustration for the notation of mixing two beams, with a shift θ between their phase fronts, on a detector in the $z = 0$ plane.

$$J_{ij}^{(\alpha)}(\boldsymbol{\rho}_1,\boldsymbol{\rho}_2,z)=\frac{I_{ij}^{(\alpha)}}{\Delta_{ij}^{(\alpha)2}(z)}\exp\left(-\frac{\boldsymbol{\rho}_1^2+\boldsymbol{\rho}_2^2}{4\sigma^{(\alpha)2}\Delta_{ij}^{(\alpha)2}(z)}\right)\exp\left(-\frac{t(\boldsymbol{\rho}_1-\boldsymbol{\rho}_2)^2}{2\delta_{ij}^{(\alpha)2}\Delta_{ij}^{(\alpha)2}(z)}\right)\times\exp\left(-\frac{\mathrm{i}k(\boldsymbol{\rho}_1^2-\boldsymbol{\rho}_2^2)}{2R_{ij}^{(\alpha)}(z)}\right),\quad(\alpha=\mathrm{S},\mathrm{L}),\ (i,j=x,y),\tag{4-1}$$

where superscripts (S) and (L) stand for the detected (signal) beam and the local oscillator beam. Formula (3-5) can be re-written in the form

$$\eta_{\mathrm{h}}=\frac{\sum_{i,j=x,y}Pc_{ij}}{\left[\sum_{i=x,y}Pd_{ii}^{(\mathrm{L})}\right]\cdot\left[\sum_{i=x,y}Pd_{ii}^{(\mathrm{S})}\right]},\tag{4-2}$$

where the coherent power of the heterodyne mixing Pc_{ij} and the incoherent power $Pd_{ii}^{(\alpha)}$ are given by the expressions

$$Pc_{ij}=\int\int_D \mathrm{Re}J_{ij}^{(\mathrm{S})*}(\boldsymbol{\rho}_1,\boldsymbol{\rho}_2,z_S)J_{ij}^{(\mathrm{L})}(\boldsymbol{\rho}_1,\boldsymbol{\rho}_2,z_L)\times\exp(\mathrm{j}\mathbf{K}\cdot\boldsymbol{\rho}_1-\mathrm{j}\mathbf{K}\cdot\boldsymbol{\rho}_2)\,\mathrm{d}^2\rho_1\,\mathrm{d}^2\rho_2,\quad(i,j)=(x,y)\tag{4-3}$$

and

$$Pd_{ii}^{(\alpha)}=\int_D J_{ii}^{\alpha}(\boldsymbol{\rho},\boldsymbol{\rho},z_{LO})\,\mathrm{d}^2\rho,\quad(i=x,y),\ \alpha=(\mathrm{L},\mathrm{S}).\tag{4-4}$$

In Eqs. (4-3) and (4-4) the symbol D indicates that the integration extends over the area of the detector with a hard-aperture of diameter D. In order to simplify the integration and following Ref. [3], it is reasonable to approximate the diameter of the hard aperture D by an aperture of radius W, sometimes called Gaussian or "soft" aperture, using the relation

$$W^2=D^2/8.\tag{4-5}$$

Next, by multiplying the integrand by the exponential cut-off factor $\exp[-(\rho_1^2+\rho_2^2)/W^2]$ and extending the integration to infinity (cf. [3]), one can rewrite Eqs. (4-3) and (4-4) in the forms

$$P_{ij}=2\mathrm{Re}\int\int_W J_{ji}^{(\mathrm{S})*}(\boldsymbol{\rho}_1,\boldsymbol{\rho}_2,z_S)J_{ij}^{(\mathrm{L})}(\boldsymbol{\rho}_1,\boldsymbol{\rho}_2,z_L)\exp\left[-\frac{\rho_1^2+\rho_2^2}{W^2}\right]\times\exp(\mathrm{j}\mathbf{K}\cdot\boldsymbol{\rho}_1-\mathrm{j}\mathbf{K}\cdot\boldsymbol{\rho}_2)\,\mathrm{d}^2\rho_1\,\mathrm{d}^2\rho_2,\quad(i,j=x,y)\tag{4-6}$$

and

$$Pd_{ii}^{(\alpha)}=\int_W J_{ii}^{(\alpha)}(\boldsymbol{\rho},\boldsymbol{\rho},z_\alpha)\exp\left[-\frac{\rho^2}{W^2}\right]\mathrm{d}^2\rho,\quad(i=x,y)\ \text{and}\ \alpha=(\mathrm{L},\mathrm{S}).\tag{4-7}$$

Using the approximation given by Eq. (4-5) and assuming that the angle θ between the wave fronts of the two overlapped beams illustrated in Fig. 4, is very small, hence $\mathbf{K}\cdot\boldsymbol{\rho}\approx k\rho\theta\cos(\phi)$, an analytic expression for the heterodyne efficiency can be derived as indicated in Appendix A. It follows from Appendix A that the analytical expressions for the coherent power of the heterodyne mixing Pc_{ij} and the incoherent power $Pd_{ii}^{(\alpha)}$ are given by

$$Pc_{ij}=(2\pi)^2\frac{I_{ij}^{(\mathrm{S})}}{\Delta_{ij}^{(\mathrm{S})2}}\frac{I_{ij}^{(\mathrm{L})}}{\Delta_{ij}^{(\mathrm{L})2}}\left(\mathrm{e}^{-\frac{F^2}{4\gamma_2}}/2\gamma_2\right)\left(\mathrm{e}^{-\frac{F^2+\beta_1^2}{4\gamma_1}}/2\gamma_1\right)\mathrm{e}^{-\left(\frac{F\beta_1}{\gamma_1}\right)},\quad(i,j)=(x,y),\tag{4-8}$$

where

$$\gamma_2=a_{ij}-\mathrm{i}b_{ij},\tag{4-9}$$

$$\eta=2c_{ij},\tag{4-10}$$

$$\gamma_1=(a_{ij}+\mathrm{i}b_{ij})+\frac{\eta^2}{4\gamma_2},\tag{4-11}$$

$$\beta_1=\frac{\eta F}{2\gamma_2},\tag{4-12}$$

$$a_{ij}=\frac{1}{\Delta_{ij}^{(\mathrm{S})2}}\left(\frac{1}{4\sigma^{(\mathrm{S})2}}+\frac{1}{2\delta_{ij}^{(\mathrm{S})2}}\right)+\frac{1}{\Delta_{ij}^{(\mathrm{L})2}}\left(\frac{1}{4\sigma^{(\mathrm{L})2}}+\frac{1}{2\delta_{ij}^{(\mathrm{L})2}}\right)+\frac{1}{W^2},\tag{4-13}$$

$$b_{ij}=\frac{k}{2}\left(\frac{1}{R_{ij}^{(\mathrm{L})}}-\frac{1}{R_{ij}^{(\mathrm{S})}}\right),\tag{4-14}$$

$$c_{ij}=\frac{1}{\delta_{ij}^{(\mathrm{S})2}\Delta_{ij}^{(\mathrm{S})2}}+\frac{1}{\delta_{ij}^{(\mathrm{L})2}\Delta_{ij}^{(\mathrm{L})2}},\tag{4-15}$$

$$F=k\theta.\tag{4-16}$$

and

$$Pd_{ii}^{\alpha}=\frac{2\pi(I_{ii}^{\alpha}/\Delta_{ii}^{(\alpha)2})}{2\left[\frac{1}{2\sigma_{ii}^{(\alpha)2}}+\frac{1}{W^2}\right]},\quad(i,j)=(x,y),\ \alpha=(\mathrm{L},\mathrm{S}).\tag{4-17}$$

We discussed the effect of the angular phase shift θ on the detection efficiency of beams of any state of coherence in another publication previously [17]. In this paper we study the effects due to propagation of electromagnetic beams; hence we consider that the two beams are co-aligned on the detector surface.

5. Results and discussion

In the following we compute the variation of the heterodyne efficiency of the coherent mixing of two stochastic beams as a function of the aperture size of the detector using Eq. (4-2). The effects of the parameters of the overlapping beams on the mixing efficiency are discussed. We begin our investigations by checking the effect of the wave-front curvature of the propagating beams on the heterodyne efficiency. For this purpose we consider the mixing of two scalar and coherent beams on the detector surface. The received beam was assumed to be scalar and coherent one with $\lambda = 0.6328$ μm and has 5 cm intensity width (σ_S), we assumed also that the beam propagated in free space for several distances (0, 1 m, 10 m). The local oscillator was chosen to be scalar and coherent with $\lambda = 0.6328$ μm, 5 cm intensity width and propagating in free space also. We assumed first that the local oscillator has planar wave-front and we checked the effect of the variation in the propagation distance of the received beam on the heterodyne efficiency as shown in Fig. 5a. One could see that when $z_S = 0$ (i.e., the received beam did not propagate) the two beams were in match and the heterodyne efficiency was unity and for small propagation distances the mismatch between the two overlapped beam was large and hence the heterodyne efficiency was less than the case of the longer propagation distance. In Fig. 5b we show the effect of the propagation of the local oscillator beam itself on the heterodyne efficiency, where we assumed $z_L = 1$ m. One can see that the mixing efficiency has been decreased due to the wave-front curvature of the local oscillator beam. As is well-known it is possible, by using a suitable lens system and adjusting the lengths before and after the lens, to compensate the wave-front curvature by the added phase from the lens [26]. We showed the importance of equalizing the phase of the propagating beams and next we will drop the effect of this wave-front curvature, assuming that the wave-front curvature has been corrected by using suitable optics in the detection system.

Next, we consider the detection of unpolarized, partially coherent beams that propagate in free space. The results for this case are shown in Fig. 6. The received beam was assumed to be unpolarized with $\lambda = 0.6328$ μm, 5 cm intensity width (σ_S), $I_{Sxx} = I_{Syy} = 0.1$, $\delta_{Sxx} = 0.1$ mm, $\delta_{Syy} = 0.5$ mm, we assumed also that the beam propagated in free space for several distances (0, 100 m, 1000 m). The local oscillator parameters were chosen as $\lambda = 0.6328$ μm, $I_{Lxx} = 1$, $I_{Lyy} = 1$, $\sigma_L = 5$ cm and we considered that the correlation widths are taking different values. In Fig. 6 we assumed that the local oscillator was fully coherent ($\delta_{Lxx} = \delta_{Lyy} = \infty$) and has correlations in two orthogonal directions. As one can see, the heterodyne efficiency in this case does not exceed the value 0.5 and it increases as the propagation distance of the received beam increases, hence according to van-Cittert Zernike theorem the coherence of the beam increases upon propagation in free space [26]. Then the matching between the two overlapping beams will increase. We checked also the effect of decreasing the correlation widths of the local oscillator beam, the heterodyne efficiency trend was the same as in Fig. 6 when we decreased the correlation widths to $\delta_{Lxx} = \delta_{Lyy} = 5$ mm. The results show that we could relax the requirement of the coherence of the local oscillator as long as its correlation width is at least 10 times larger than the corresponding correlation width of the received beam.

Finally, we checked the case of the detection of partially polarized, partially coherent beams as given in Fig. 7. The parameters of the received beam were assumed to be $\lambda = 0.6328$ μm, $\sigma_S = 5$ cm, $I_{Sxx} = I_{Syy} = 0.5$, $I_{Sxy} = 0.125$, $\delta_{Sxx} = \delta_{Syy} = 0.1$ mm, $\delta_{Sxy} = 0.5$ mm, we assumed also that the beam propagated in free space for several distances (0, 100 m, 1000 m). The local oscillator parameters were chosen as $\lambda = 0.6328$ μm, $I_{Lxx} = I_{Lyy} = I_{Lxy} = 5$, $\sigma_L = 5$ cm and we considered that correlation widths are equal as the case for the fully

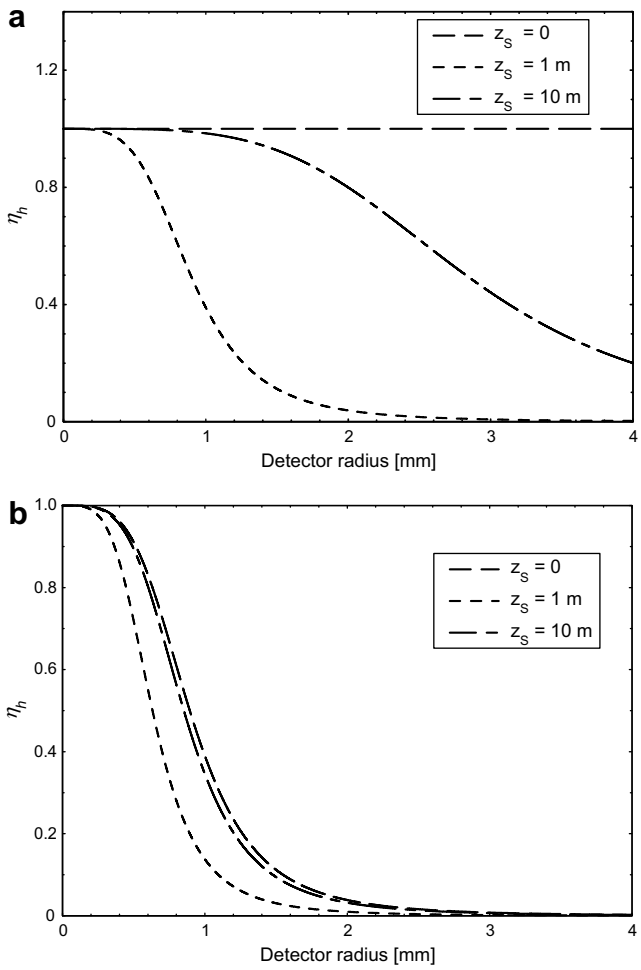

Fig. 5. Variation of the heterodyne efficiency (η_h) with the detector radius, the received beam was assumed to be scalar and coherent with $\lambda = 0.6328$ μm and has 5 cm intensity width (σ) and propagating for a distance 0, 1 m, 10 m in free space. The local oscillator was chosen to be scalar and coherent with $\lambda = 0.6328$ μm, 5 cm intensity width and propagating for a distance (a) 0 (b) 1 m in free space.

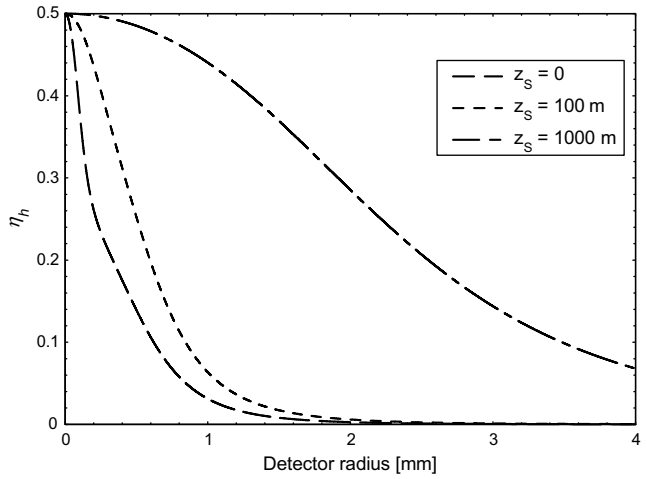

Fig. 6. Variation of the heterodyne efficiency (η_h) with the detector radius. The received beam was assumed to be unpolarized with $\lambda = 0.6328$ μm, 5 cm intensity width (σ_S), $I_{Sxx} = I_{Syy} = 0.1$, $\delta_{Sxx} = 0.1$ mm, $\delta_{Syy} = 0.5$ mm and propagating for a distance 0, 100 m, 1000 m in free space. The local oscillator parameters were chosen as $\lambda = 0.6328$ μm, $I_{Lxx} = 1$, $I_{Lyy} = 1$, $\sigma_L = 5$ cm and $\delta_{Lxx} = \delta_{Lyy} = \infty$.

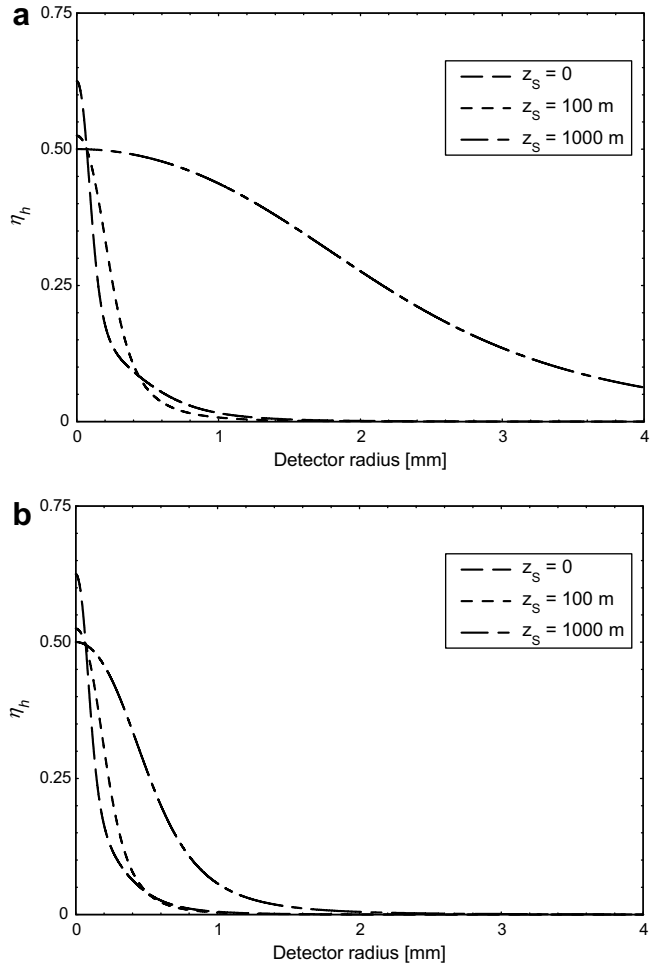

Fig. 7. Variation of the heterodyne efficiency (η_h) with the detector radius. The parameters of the received beam were assumed to be $\lambda = 0.6328$ μm, $\sigma_S = 5$ cm, $I_{Sxx} = I_{Syy} = 0.5$, $I_{Sxy} = 0.125$, $\delta_{Sxx} = \delta_{Syy} = 0.1$ mm, $\delta_{Sxy} = 0.5$ mm and propagating distance $z_S = 0$, 100 m, 1000 m in free space. The local oscillator parameters were chosen as fully polarized beam has $\lambda = 0.6328$ μm, $I_{Lxx} = I_{Lyy} = I_{Lxy} = 5$, $\sigma_L = 5$ cm and (a) $\delta_{Lxx} = \delta_{Lyy} = \delta_{Lxy} = \infty$ (b) $\delta_{Lxx} = \delta_{Lyy} = \delta_{Lxy} = 0.5$ mm.

polarized GSM beam but they are taking different values in each figure. In Fig. 7a we assumed that the local oscillator is coherent as we chose $\delta_{Lxx} = \delta_{Lyy} = \delta_{Lxy} = \infty$. One can see that as the beam propagate in free-space the heterodyne efficiency becomes more homogeneous over larger aperture size but its magnitude reduces due to free-space diffraction. The aperture averaging does not improve the performance of the detection system as shown. We checked also the effect of decreasing the correlation widths of the local oscillator beam, the heterodyne efficiency trend was the same as in Fig. 7a when we decreased the correlation widths to $\delta_{Lxx} = \delta_{Lyy} = 5$ mm. Hence one could relax the requirement of the coherence of the local oscillator by using a suitable partially coherent beam. In Fig. 7b we assumed that $\delta_{Lxx} = \delta_{Lyy} = \delta_{Lxy} = 0.5$ mm. As is clear in the figure the heterodyne efficiency decreased significantly with respect to the results seen previously in Fig. 7a. One can see that, when we decreased the correlation widths of the local oscillator to unacceptable degree, as in this example, the heterodyne efficiency deteriorated drastically.

6. Conclusions

An expression for the heterodyne efficiency of mixing two stochastic electromagnetic beams with a small angular shift between their propagation directions has been derived as a measure for the quality of the coherent mixing of such beams. The effect of the change of the beams parameters in free-space has been considered. We derived an analytical expression for the heterodyne efficiency for the case of mixing two stochastic electromagnetic Gaussian Schell-model (GSM) beams. The numerical examples demonstrate that the heterodyne efficiency of the coherent detection could be adjusted by controlling the corresponding parameters of the local oscillator beam parameters. We have also shown by some examples that the optimal values for the parameters of the local oscillator beam depend on specific characteristics of the detected beam.

Acknowledgements

We would like to thank Prof. Emil Wolf, University of Rochester, for helpful comments related to the topic presented in this paper. We would like to thank Prof. Larry Andrews, University of Central Florida for his helpful suggestions related to the mathematical analysis given in Appendix A. This work benefited from the support of the Florida Photonics Center of Excellence (FPCE).

Appendix A

In this Appendix we give details of the analytical solution for the heterodyne efficiency of GSM beams. We begin by performing the integration

$$P_{cij} = \frac{2I_{ij}^{(S)}I_{ij}^{(L)}}{\Delta_{ij}^{(S)2}\Delta_{ij}^{(LO)2}}\mathrm{Re}\int\int_W \exp\left(-\frac{\rho_1^2+\rho_2^2}{4\sigma^{(S)2}\Delta_{ij}^{(S)2}}\right)\exp\left(-\frac{(\boldsymbol{\rho}_1-\boldsymbol{\rho}_2)^2}{2\delta_{ij}^{(S)2}\Delta_{ij}^{(S)2}}\right)$$
$$\times\exp\left(\frac{\mathrm{i}k(\rho_1^2-\rho_2^2)}{2R_{ij}^{(S)}}\right)\exp\left(-\frac{\rho_1^2+\rho_2^2}{4\sigma^{(L)2}\Delta_{ij}^{(L)2}}\right)\exp\left(-\frac{(\boldsymbol{\rho}_1-\boldsymbol{\rho}_2)^2}{2\delta_{ij}^{(L)2}\Delta_{ij}^{(L)2}}\right)$$
$$\times\exp\left(-\frac{\mathrm{i}k(\rho_1^2-\rho_2^2)}{2R_{ij}^{(L)}}\right)\exp\left[-\frac{\rho_1^2+\rho_2^2}{W^2}\right]$$
$$\times\exp j(\mathbf{K}\cdot\boldsymbol{\rho}_1-\mathrm{j}\mathbf{K}\cdot\boldsymbol{\rho}_2)\,\mathrm{d}^2\rho_1\,\mathrm{d}^2\rho_2,\quad (i,j=x,y). \tag{A1}$$

This formula can be compactly written as

$$P_{cij} = \frac{2I_{ij}^{(S)}I_{ij}^{(L)}}{\Delta_{ij}^{(S)2}\Delta_{ij}^{(L)2}}\mathrm{Re}\int_W \exp[-(a_{ij}+\mathrm{i}b_{ij})\rho_1^2]\rho_1\,\mathrm{d}\phi_1\,\mathrm{d}\rho_1$$
$$\times\int_W \exp[-(a_{ij}-\mathrm{i}b_{ij})\rho_2^2]\exp[c_{ij}\rho_1\rho_2\cos(\phi_1-\phi_2)]$$
$$\times\exp(\mathrm{j}k\rho_1\theta\cos\phi_1-\mathrm{j}k\rho_2\theta\cos\phi_2)\rho_2\,\mathrm{d}\phi_2\,\mathrm{d}\rho_2,\quad (i,j=x,y), \tag{A2}$$

where the coefficients a_{ij}, b_{ij} and c_{ij} are

$$a_{ij} = \frac{1}{\Delta_{ij}^{(S)2}}\left(\frac{1}{4\sigma^{(S)2}}+\frac{1}{2\delta_{ij}^{(S)2}}\right)$$
$$+\frac{1}{\Delta_{ij}^{(L)2}}\left(\frac{1}{4\sigma^{(L)2}}+\frac{1}{2\delta_{ij}^{(L)2}}\right)+\frac{1}{W^2}, \tag{A3}$$

$$b_{ij} = \frac{k}{2}\left(\frac{1}{R_{ij}^{(L)}}-\frac{1}{R_{ij}^{(S)}}\right), \tag{A4}$$

$$c_{ij} = \frac{1}{\delta_{ij}^{(S)2}\Delta_{ij}^{(S)2}}+\frac{1}{\delta_{ij}^{(L)2}\Delta_{ij}^{(L)2}}. \tag{A5}$$

Let us denote also $F = k\theta$, $F' = \mathrm{i}k\theta$ and $C_{ij} = c_{ij}\rho_1\rho_2$. The integration may be written as

$$P_{cij} = \int_{\rho_1=0}^{\infty}\int_{\rho_2=0}^{\infty}\int_{\phi_2=0}^{2\pi}\int_{\phi_1=0}^{2\pi}\mathrm{Re}[I_{ij}^{(S)}I_{ij}^{(L)}\mathrm{e}^{-(a_{ij}+\mathrm{i}b_{ij})\rho_1^2}\mathrm{e}^{-(a_{ij}-\mathrm{i}b_{ij})\rho_2^2}\mathrm{e}^{C_{ij}\cos(\phi_1-\phi_2)}]$$
$$\times[\mathrm{e}^{F'(\rho_1\cos\phi_1-\rho_2\cos\phi_2)}]\rho_1\rho_2\,\mathrm{d}\phi_1\,\mathrm{d}\phi_2\,\mathrm{d}\rho_2\,\mathrm{d}\rho_1. \tag{A6}$$

To evaluate P_{cij}, we perform the integration over ϕ_1 and by rearranging the terms of P_{cij} one finds

$$I = \int_{\rho_1=0}^{\infty}\int_{\rho_2=0}^{\infty}\int_{\phi_2=0}^{2\pi} \mathrm{Re}[I_{ij}^{(S)} I_{ij}^{(L)} \mathrm{e}^{-(a_{ij}+\mathrm{i}b_{ij})\rho_1^2} \mathrm{e}^{-(a_{ij}-\mathrm{i}b_{ij})\rho_2^2} \mathrm{e}^{-F'\rho_2\cos\phi_2}] \times \rho_1\rho_2\,\mathrm{d}\phi_2\,\mathrm{d}\rho_2\,\mathrm{d}\rho_1 \int_{\phi_1=0}^{2\pi} \mathrm{e}^{[\cos\phi_1(C_{ij}\cos\phi_2+F'\rho_1)-\sin\phi_1(C_{ij}\sin\phi_2)]}\,\mathrm{d}\phi_1. \tag{A7}$$

Using the identities ([27,28])

$$\int_{\phi=0}^{2\pi} \mathrm{e}^{[\alpha\cos\phi+\beta\sin\phi]}\,\mathrm{d}\phi = 2\pi I_0\left(\sqrt{\alpha^2+\beta^2}\right), \tag{A8}$$

$$I_0\left(\sqrt{N^2+M^2-2MN\cos(\phi_2-\psi)}\right) = \sum_{-\infty}^{\infty}(-1)^m I_m(N) I_m(M)\cos m(\phi_2-\psi), \tag{A9}$$

where I_m is the modified Bessel function of order m and $\psi = \pi$. The integration gives

$$P_{cij} = 2\pi\sum_{-\infty}^{\infty}(-1)^m \int_{\rho_1=0}^{\infty}\int_{\rho_2=0}^{\infty} \mathrm{Re}[I_{ij}^{(S)} I_{ij}^{(L)} \mathrm{e}^{-(a_{ij}+\mathrm{i}b_{ij})\rho_1^2} \mathrm{e}^{-(a_{ij}-\mathrm{i}b_{ij})\rho_2^2}] \times I_m(C_{ij}) I_m(F'\rho_1)\rho_1\rho_2\,\mathrm{d}\rho_2\,\mathrm{d}\rho_1 \times \int_{\phi_2=0}^{2\pi} \mathrm{e}^{[F'\rho_2\cos\phi_2]}\cos m(\phi_2-\psi)\,\mathrm{d}\phi_2. \tag{A10}$$

By using the identity [28]

$$\int_{\phi=0}^{2\pi} \mathrm{e}^{[\alpha\cos\phi+\beta\sin\phi]}\cos m(\phi-\psi)\,\mathrm{d}\phi = 2\pi I_m(\sqrt{\alpha^2+\beta^2})\cos m(\phi-\xi), \tag{A11}$$

where $\xi = \tan^{-1}(\frac{\beta}{\alpha})$, the integral becomes

$$P_{cij} = (2\pi)^2 \sum_{-\infty}^{\infty}(-1)^m \cos(m\psi) \times \int_{\rho_1=0}^{\infty}\int_{\rho_2=0}^{\infty} \mathrm{Re}[I_{ij}^{(S)} I_{ij}^{(L)} \mathrm{e}^{-(a_{ij}+\mathrm{i}b_{ij})\rho_1^2} \mathrm{e}^{-(a_{ij}-\mathrm{i}b_{ij})\rho_2^2}] I_m(C_{ij}) I_m(F'\rho_1) \times I_m(F'\rho_2)\rho_1\rho_2\,\mathrm{d}\rho_2\,\mathrm{d}\rho_1. \tag{A12}$$

By substituting the value of the modified Bessel function of order m in terms of Bessel function [27] one has

$$I_m(F'\rho_1) = j^{-m} J_m(-F\rho_1), \tag{A13}$$

$$I_m(F'\rho_2) = j^{-m} J_m(-F\rho_2). \tag{A14}$$

The integral can be written as

$$P_{cij} = (2\pi)^2 I_{ij}^{(S)} I_{ij}^{(L)} \sum_{-\infty}^{\infty}(-1)^m \cos(m\psi) \int_{\rho_1=0}^{\infty} \mathrm{Re}\,\mathrm{e}^{-(a_{ij}+\mathrm{i}b_{ij})\rho_1^2} J_m(-F\rho_1)\rho_1\,\mathrm{d}\rho_1 \times \int_{\rho_2=0}^{\infty} \rho_2 \mathrm{e}^{-(a_{ij}-\mathrm{i}b_{ij})\rho_2^2} J_m(F\rho_2) I_m(2c_{ij}\rho_1\rho_2)\,\mathrm{d}\rho_2. \tag{A15}$$

The integration over ρ_2 can be performed by using the identity [29]

$$\int_{x=0}^{\infty} x\mathrm{e}^{-\alpha x^2} I_l(\gamma x)\,\mathrm{d}x = \frac{1}{2\alpha}\mathrm{e}^{\frac{(\beta^2-\gamma^2)}{4\alpha}} J_l\left(\frac{\beta\gamma}{2\alpha}\right). \tag{A16}$$

The integral becomes

$$P_{cij} = (2\pi)^2 I_{ij}^{(S)} I_{ij}^{(L)} \left(\mathrm{e}^{-\frac{F'^2}{4\gamma_2}}/2\gamma_2\right) \sum_{m=-\infty}^{\infty}(-1)^m \cos(m\psi) \times \int_{\rho_1=0}^{\infty} \mathrm{e}^{-((a_{ij}+\mathrm{i}b_{ij})+\frac{\eta^2}{4\gamma_2})\rho_1^2} J_m(-F\rho_1) J_m\left(-\frac{\eta F}{2\gamma_2}\right)\rho_1\,\mathrm{d}\rho_1, \tag{A17}$$

where

$$\gamma_2 = a_{ij} - \mathrm{i}b_{ij}, \tag{A18}$$

$$\eta = 2c_{ij}. \tag{A19}$$

The integration over r_1 can be performed, using the identity [29]

$$\int_{x=0}^{\infty} x\mathrm{e}^{-\mu^2x^2} J_l(\alpha x) J_l(\beta x)\,\mathrm{d}x = \frac{1}{2\mu^2}\mathrm{e}^{\frac{(\alpha^2+\beta^2)}{4\mu^2}} I_l\left(\frac{\beta\gamma}{2\mu^2}\right), \tag{A20}$$

and one finds that

$$P_{cij} = (2\pi)^2 I_{ij}^{(S)} I_{ij}^{(L)} \left(\mathrm{e}^{-\frac{F^2}{4\gamma_2}}\Big/2\gamma_2\right)\left(\mathrm{e}^{-\frac{F^2+\beta_1^2}{4\gamma_1}}\Big/2\gamma_1\right) \times \sum_{m=-\infty}^{\infty}(-1)^m \cos(m\psi) I_m\left(\frac{F\beta_1}{\gamma_1}\right), \tag{A21}$$

where

$$\gamma_1 = (a_{ij}+\mathrm{i}b_{ij}) + \frac{\eta^2}{4\gamma_2}, \tag{A22}$$

$$\beta_1 = \frac{\eta F}{2\gamma_2}. \tag{A23}$$

Finally using the identity [28]

$$\sum_{m=-\infty}^{\infty}(-1)^m I_m\left(\frac{F\beta_1}{\gamma_1}\right)\cos(m\psi) = \mathrm{e}^{\frac{F\beta_1}{\gamma_1}\cos(\psi)}. \tag{A24}$$

The integral P_{cij} can be written in closed form

$$P_{cij} = (2\pi)^2 I_{ij}^{(S)} I_{ij}^{(L)} \left(\mathrm{e}^{-\frac{F^2}{4\gamma_2}}\Big/2\gamma_2\right)\left(\mathrm{e}^{-\frac{F^2+\beta_1^2}{4\gamma_1}}\Big/2\gamma_1\right)\mathrm{e}^{-\left(\frac{F\beta_1}{\gamma_1}\right)}. \tag{A25}$$

The integrals in the denominator of Eq. (22) take the form

$$P_d = \int_{\phi=0}^{2\pi}\int_{\rho=0}^{\infty} \Gamma(\boldsymbol{\rho},\boldsymbol{\rho})\mathrm{e}^{-\frac{\rho^2}{W^2}}\rho\,\mathrm{d}\rho\,\mathrm{d}\phi. \tag{A26}$$

For Gaussian mutual coherence function case, one expresses the integral as follows:

$$P_d = \int_{\phi=0}^{2\pi}\int_{\rho=0}^{\infty} I\mathrm{e}^{-(\frac{\rho^2}{2\sigma^2})}\mathrm{e}^{-\frac{\rho^2}{W^2}}\rho\,\mathrm{d}\rho\,\mathrm{d}\phi. \tag{A27}$$

Integrating over ϕ one finds that

$$P_d = 2\pi I\int_{\rho=0}^{\infty} \mathrm{e}^{-(\frac{\rho^2}{2\sigma^2})}\mathrm{e}^{-\frac{\rho^2}{W^2}}\rho\,\mathrm{d}\rho\,\mathrm{d}\phi. \tag{A28}$$

The integration over r can be performed using the identity [29]

$$\int_{x=0}^{\infty} x\mathrm{e}^{-\mu^2x^2}\,\mathrm{d}x = \frac{1}{2\mu^2}. \tag{A29}$$

Hence the integral can be expressed in closed form as

$$P_d = \frac{2\pi I}{2\left[\frac{1}{2\sigma^2}+\frac{1}{W^2}\right]}. \tag{A30}$$

References

[1] G.R. Osche, Optical Detection Theory, John Wiley & Sons Inc., 2002.
[2] R.C. Coutinho, H.A. French, D.R. Selviah, D. Wickramasinghe, H.D. Griffiths, in: IEEE Lasers and Electro-Optics Society 12th Annual Meeting, 1999, p. 227.
[3] L.C. Andrews, R.L. Phillips, C.Y. Hopen, Laser Beam Scintillation with Applications, SPIE Press, Bellingham, 2001.
[4] J.H. McElroy, Appl. Opt. 11 (1972) 1619.
[5] M.M. Abbas, M.J. Mumma, T. Kostiuk, D. Buhl, Appl. Opt. 15 (1976) 427.
[6] L. Mandel, E. Wolf, J. Opt. Soc. Am. 65 (1975) 413.
[7] A. Siegman, Appl. Opt. 5 (1966) 1588.
[8] D. Fink, Appl. Opt. 14 (1975) 689.
[9] J. Lathi, Appl. Opt. 8 (1969) 1815.
[10] J. Lathi, C. Nagel, Appl. Opt. 9 (1970) 115.
[11] M. Salem, A. Dogariu, J. Mod. Opt. 51 (2004) 2305.

[12] Y. Zhao, M.J. Post, R.M. Haresty, Appl. Opt. 29 (1990) 4111.
[13] R.G. Frehlich, J. Mod. Opt. 41 (1994) 2115.
[14] S.C. Cohen, Appl. Opt. 14 (1975) 1953.
[15] K. Tanaka, N. Ohta, Appl. Opt. 26 (1987) 627.
[16] K. Tanaka, N. Saga, Appl. Opt. 23 (1984) 3901.
[17] M. Salem, The Effects of Polarization and Coherence on the Propagation and the Detection of Stochastic Electromagnetic Beams, Doctoral dissertation, University of Central Florida, United States, 2007.
[18] S.R. Seshadri, J. Appl. Phys. 87 (2000) 4084.
[19] F. Gori, M. Santarsiero, S. Vicalvi, R. Borghi, G. Guattari, J. Opt. A: Pure Appl. Opt. 7 (1998) 941.
[20] F. Gori, M. Santarsiero, G. Piquero, R. Borghi, A. Mondello, R. Simon, J. Opt. A: Pure Appl. Opt. 3 (2001) 1.
[21] E. Collett, Polarized Light: Fundamentals and Applications, Marcel Dekker Inc., 1993.
[22] O. Korotkova, E. Wolf, Opt. Commun. 246 (2005) 35.
[23] G. Piquero, P. Romanini, F. Gori, M. Santarsiero, R. Borghi, A. Mandello, Opt. Commun. 208 (2002) 9.
[24] T. Shirai, O. Korotkova, E. Wolf, J. Opt. A: Pure Appl. Opt. 7 (2005) 232.
[25] H.T. Yura, Appl. Opt. 13 (1974) 150.
[26] M. Born, E. Wolf, Principles of Optics, seventh ed., Cambridge University Press, Cambridge, 1999.
[27] L.C. Andrews, R.L. Phillips, Laser Beam Propagation Through Random Media, SPIE Optical Engineering Press, Bellingham, WA, 1998.
[28] G.N. Watson, A Treatise on the Theory of Bessel Functions, Cambridge, New York, 1962.
[29] I.S. Gradshteyn, I.M. Ryzhik, Table of Integrals, Series, and Products, Scripta Technica, Inc., Transl., Academic Press, New York, 1965.